Supporting Information

Structural Characterization of Bio-Functionalized Gold Nanoparticles by Ultrahigh Resolution Mass Spectrometry

Simone Nicolardi[1]*, Yuri E.M. van der Burgt[1], Jeroen D.C. Codée[2], Manfred Wuhrer[1], Cornelis H. Hokke[3], Fabrizio Chiodo[2,3]*.

1. Center for Proteomics and Metabolomics, Leiden University Medical Center, Leiden, The Netherlands

2. Department of Bio-Organic Synthesis, Leiden Institute of Chemistry, Leiden, The Netherlands

3. Department of Parasitology, Leiden University Medical Center, Leiden, The Netherlands

Table of contents

Figure S1	LDI- and LDI/MALDI-TOF MS of OVA peptide AuNPs	S2
Figure S2	MS/MS analysis of AuNPs with OVA 323–339 peptide-based ligand	S3
Figure S3	Scheme of b-type and y-type fragmentation during CID	S4
Figure S4	MS/MS spectra of $[M\text{-}SH_2+H]^+$ (A) and $[M\text{-}S+H]^+$ (B) generated from OVA peptide AuNPs	S5
Figure S5	MS/MS spectrum of the OVA peptide ligand linked to the glucose ligand via a S-S bond	S6
Figure S6	MS analysis of OVA peptide AuNPs using either 1,5-DAN (A) or sinapinic acid (B) as MALDI matrix	S7
Figure S7	MS/MS analysis of pseudo-molecular ions (A-H) generated from Glu-C digested OVA peptide AuNPs	S8
Figure S8	MS/MS analysis of pseudo-molecular ions (A-E) generated from Lewis X AuNPs	S9
Figure S9	MS analysis of Lewis X ligand not linked to AuNPs	S10
Figure S10	MS/MS analysis of pseudo-molecular ions (A-B) generated from tetramannoside AuNPs	S11
Figure S11	MS spectrum of tetramannoside AuNPs analysed without NaCl	S12
	Experimental conditions for the synthesis of each NP and supporting structural information.	S13

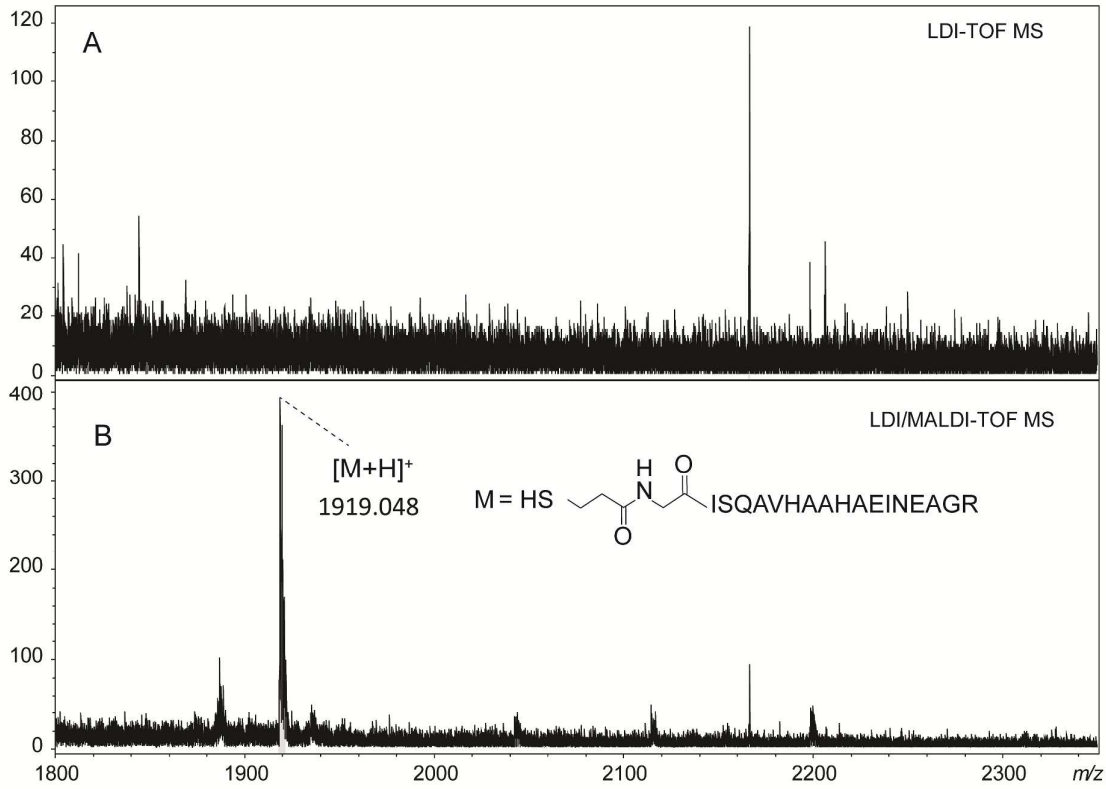

Figure S1. Relevant parts of the TOF mass spectra of AuNPs with OVA 323–339 peptide-based ligand obtained from LDI only (A) and LDI/MALDI (B).

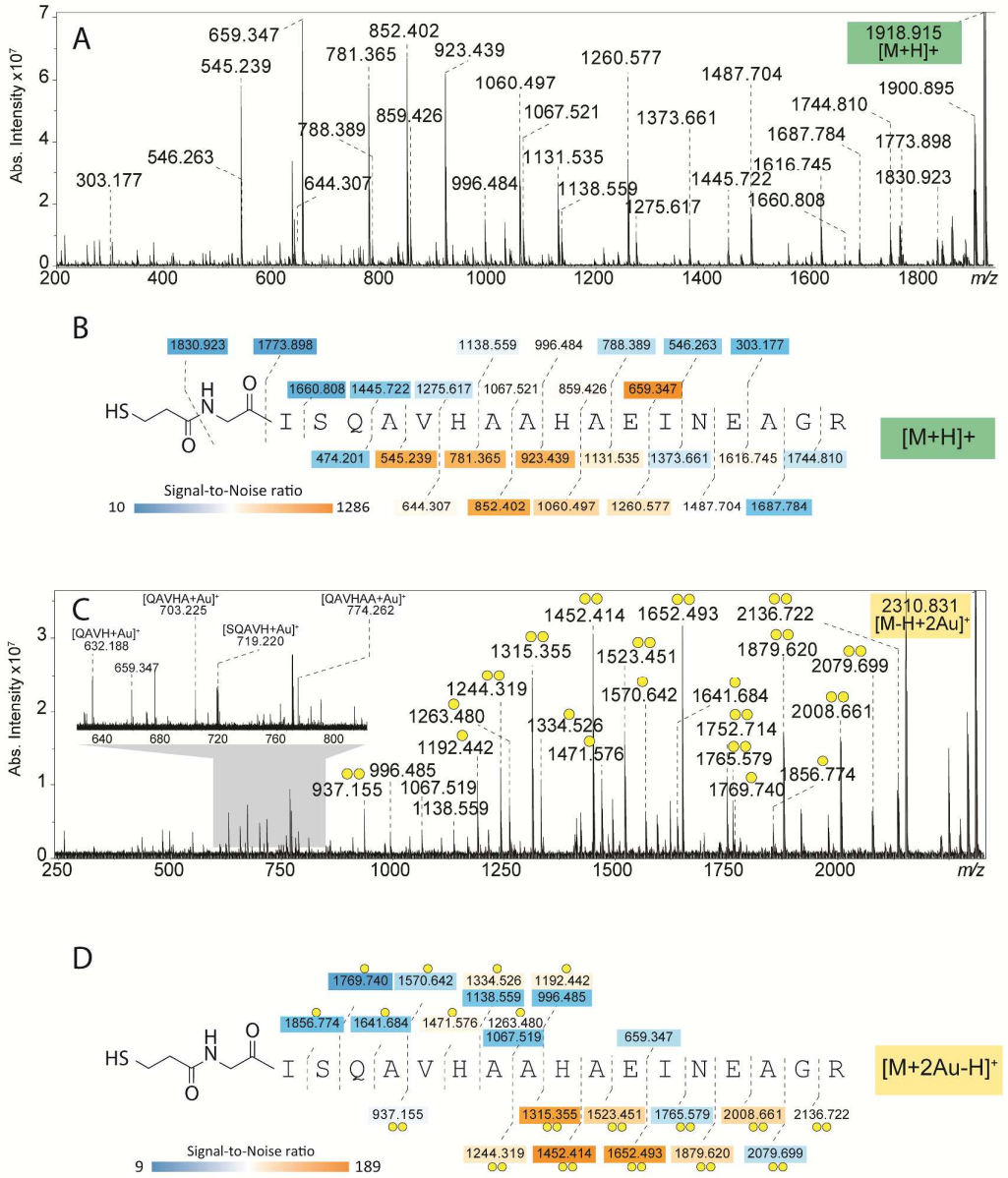

Figure S2. MS/MS analysis of AuNPs with OVA 323–339 peptide-based ligand. Structure characterization of $[M+H]^+$ and $[M+2Au-H]^+$ by collision-induced dissociation (CID) resulted in tandem mass spectra A and C with corresponding sequence coverages depicted in B and D.

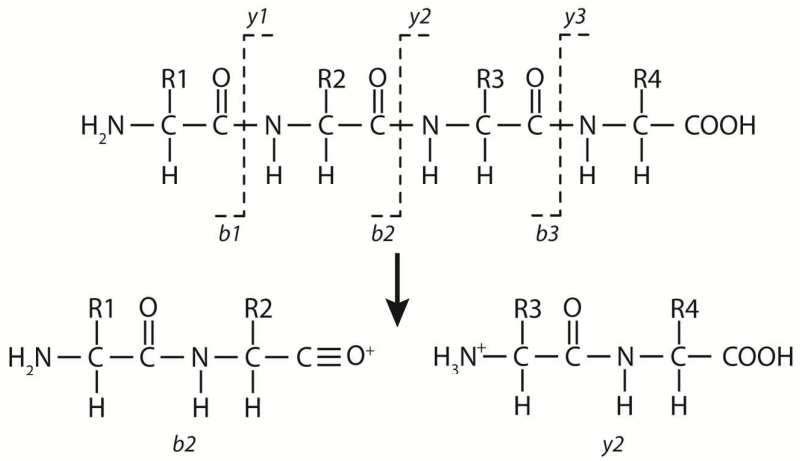

Figure S3. During CID, b-type and y-type fragments are generated from the cleavage of the peptide bond. If the charge is retained on the C-terminal part, y-type ions are formed while if the charge is retained on the N-terminal part, b-type ions are formed (Klaus Biemann Biological Mass Spectrometry 1988, 16, 99-111).

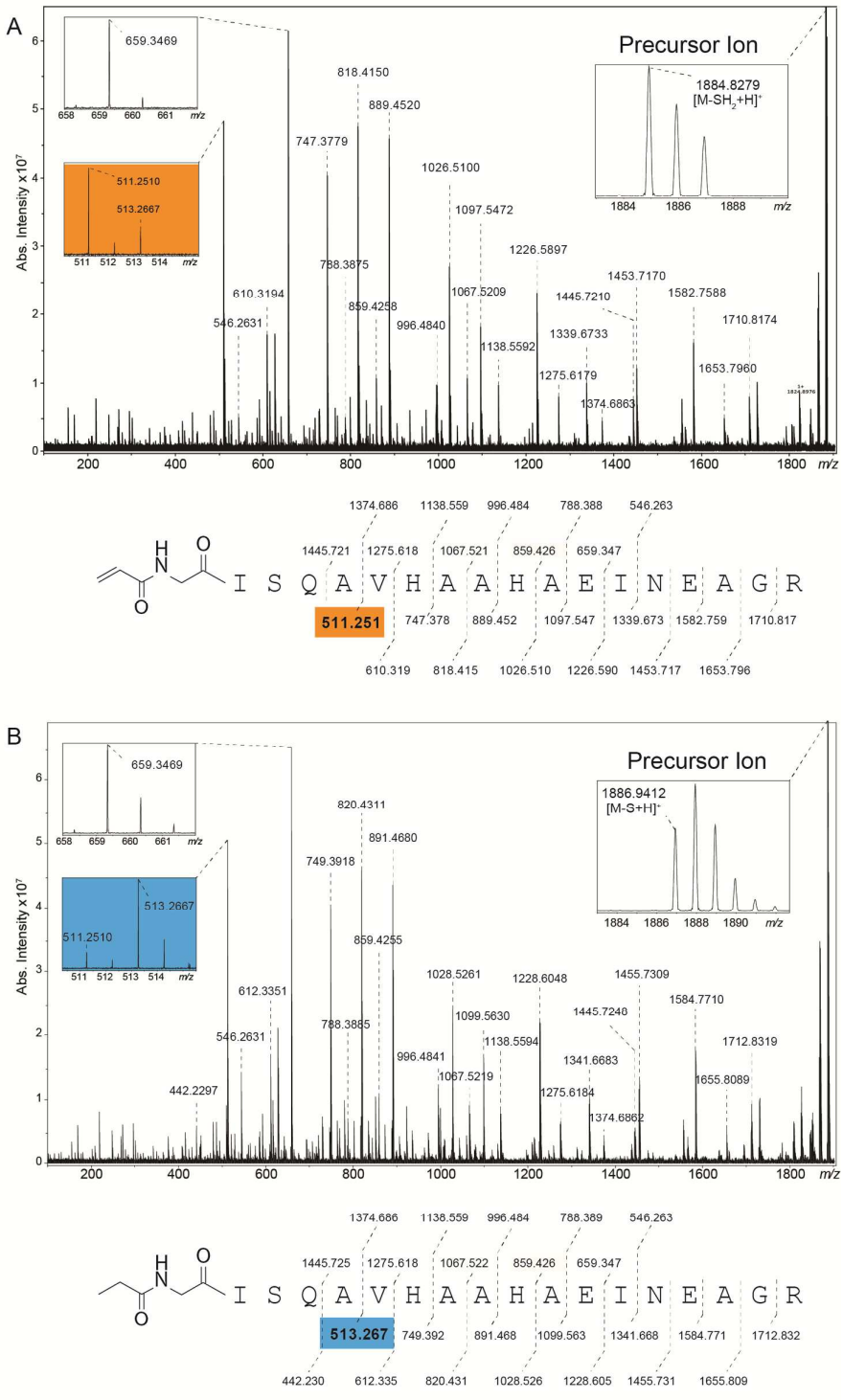

Figure S4. LDI/MALDI-CID-FTICR MS/MS spectra of $[M\text{-}SH_2+H]^+$ (A) and $[M\text{-}S+H]^+$ (B) generated from OVA peptide AuNPs. The b-type fragments detected at *m/z* 511.2510 and *m/z* 513.2667 were diagnostic for $[M\text{-}SH_2+H]^+$ and $[M\text{-}S+H]^+$, respectively.

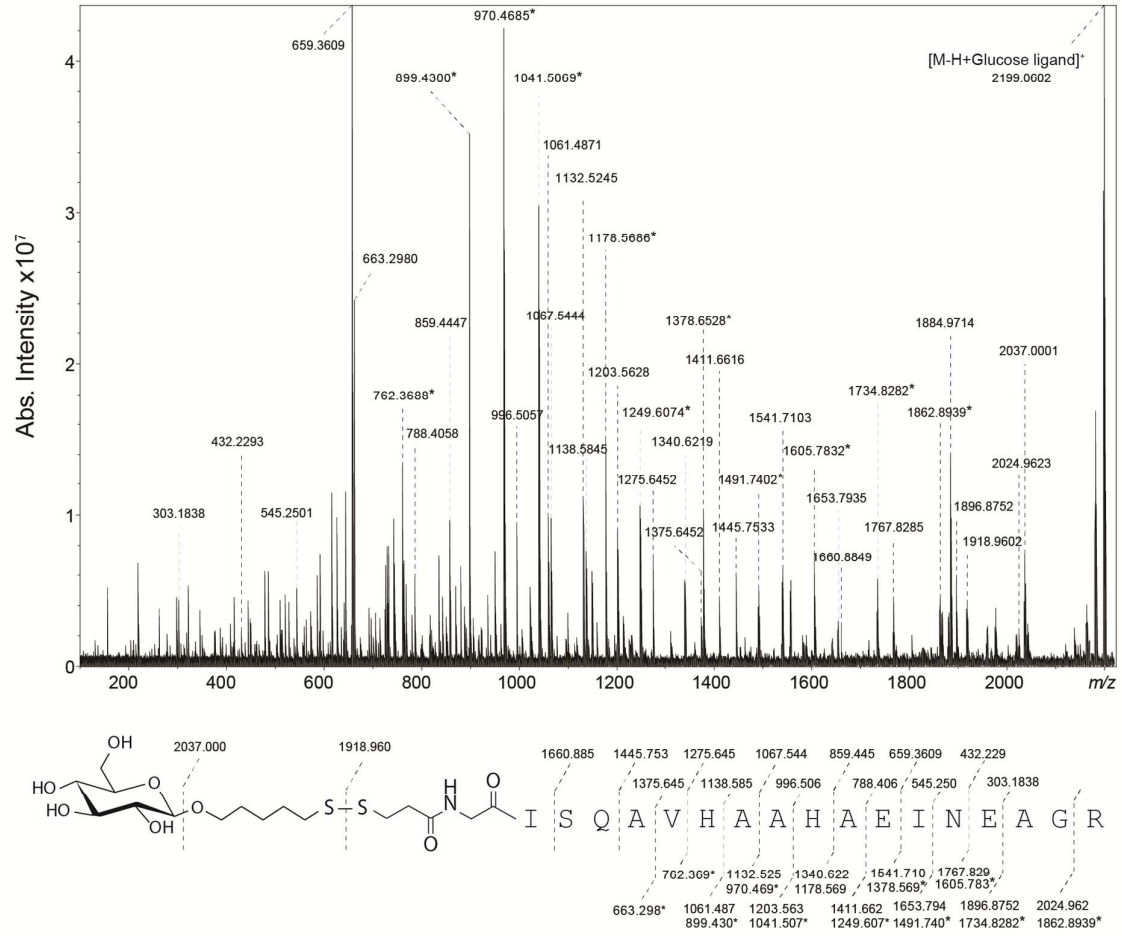

Figure S5. LDI/MALDI-CID-FTICR MS/MS spectrum of the OVA peptide ligand linked to the glucose ligand via a S-S bond. * Internal fragments without glucose.

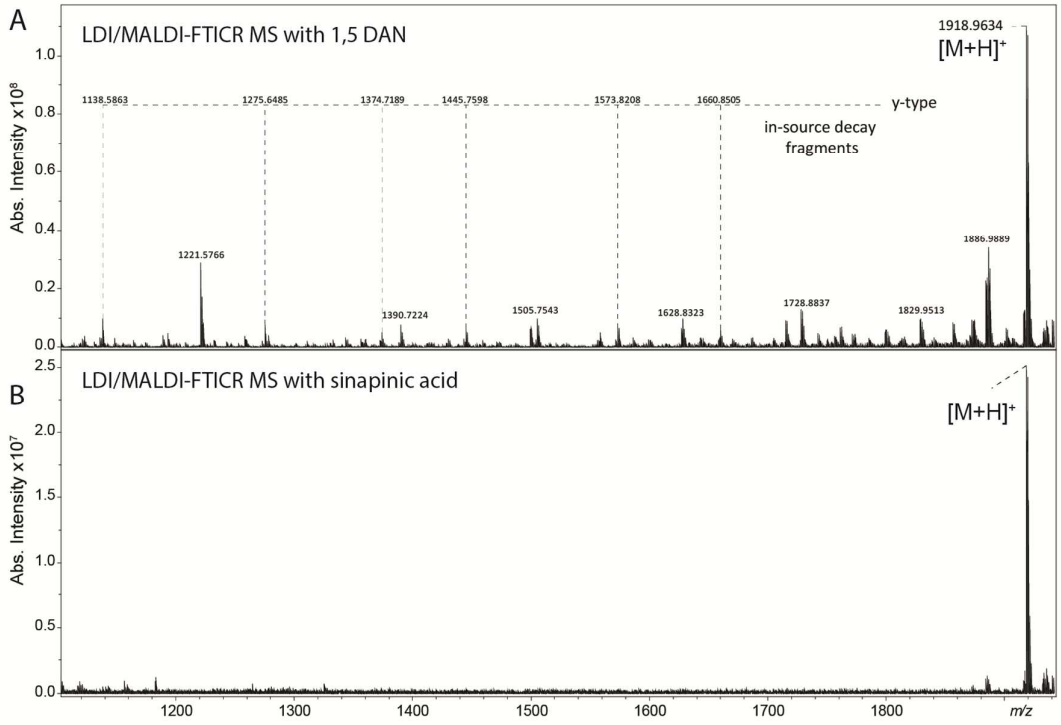

Figure S6. LDI/MALDI-FTICR MS spectra generated from the analysis of OVA peptide AuNPs using either 1,5-DAN (A) or sinapinic acid (B) as MALDI matrix.

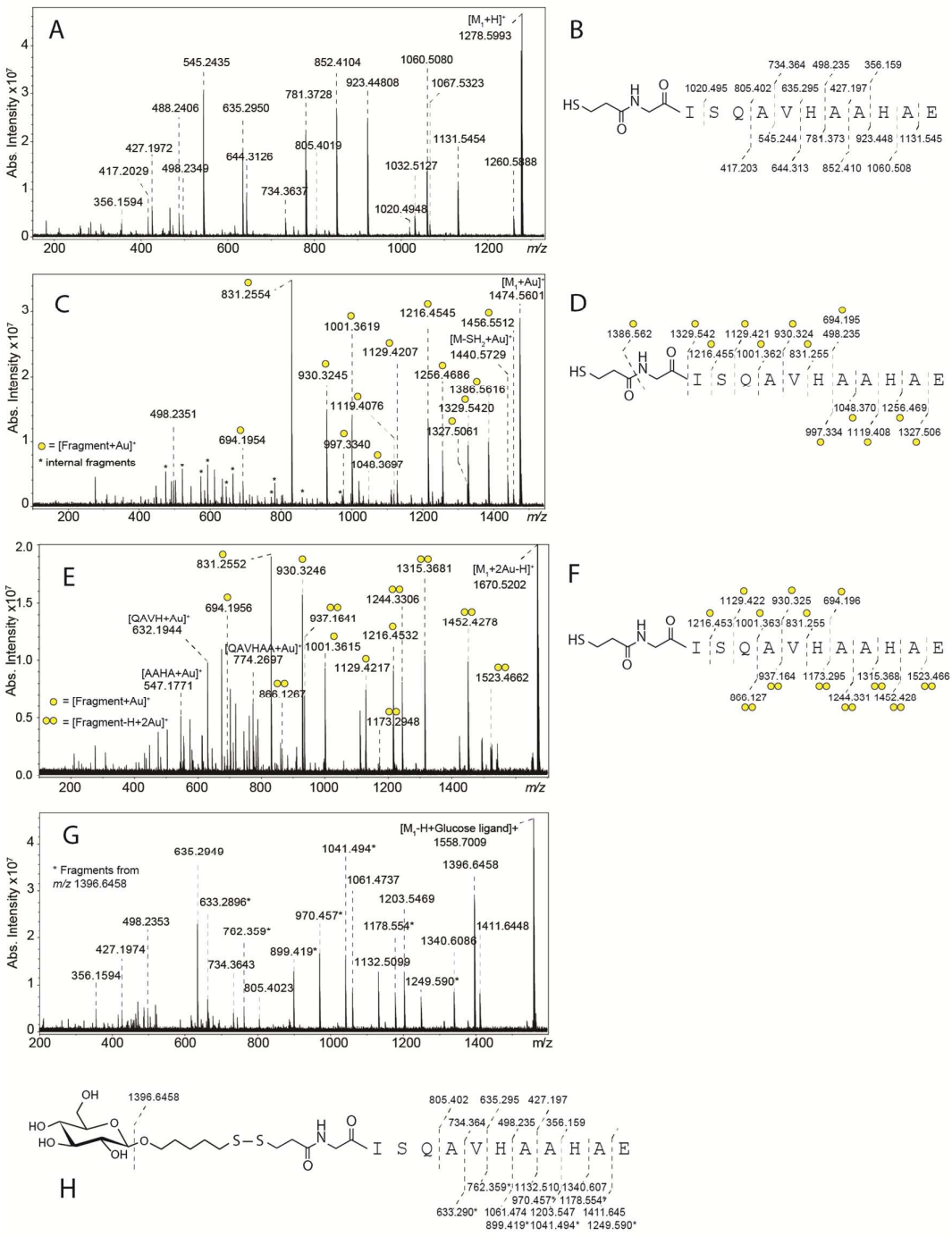

Figure S7. LDI/MALDI-CID-FTICR MS/MS spectra and sequence coverage obtained from (A, B) $[M_1+H]^+$, (C, D) $[M_1+Au]^+$, (E, F) $[M_1+2Au-H]^+$ and (G, H) $[M_1-H+Glucose\ ligand]^+$ generated by LDI/MALDI-FTICR MS of Glu-C digested OVA peptide AuNPs. Yellow circles indicate gold-linked fragment ions.

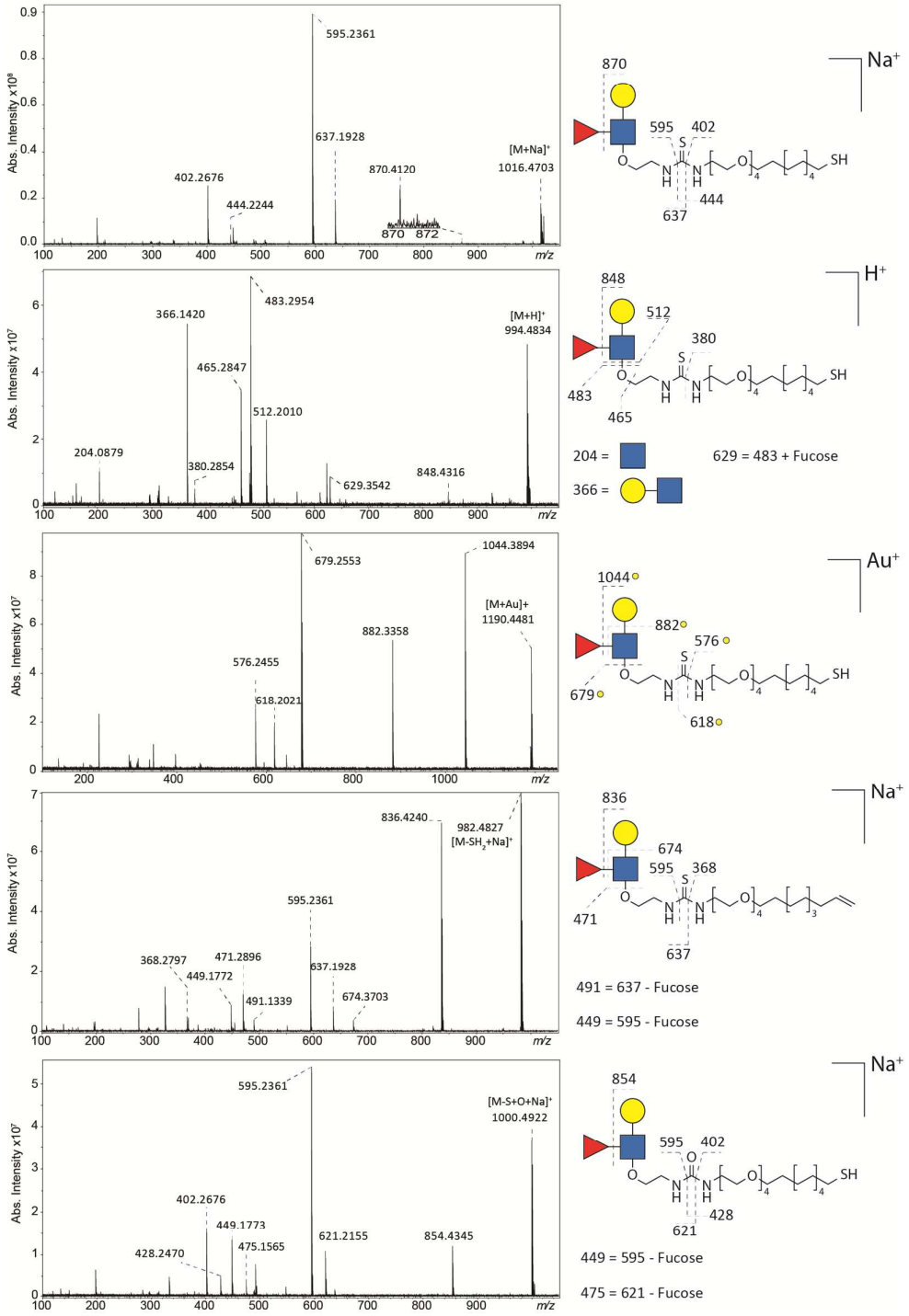

Figure S8. LDI/MALDI-CID-FTICR MS/MS spectra and structural characterization of (A) $[M+Na]^+$, (B)$[M+H]^+$, (C) $[M+Au]^+$, (D) $[M-SH_2+Na]^+$ and (E) $[M-S+O+Na]^+$ generated by LDI/MALDI-FTICR MS of Lewis X AuNPs. Yellow circles indicate gold-linked fragment ions.

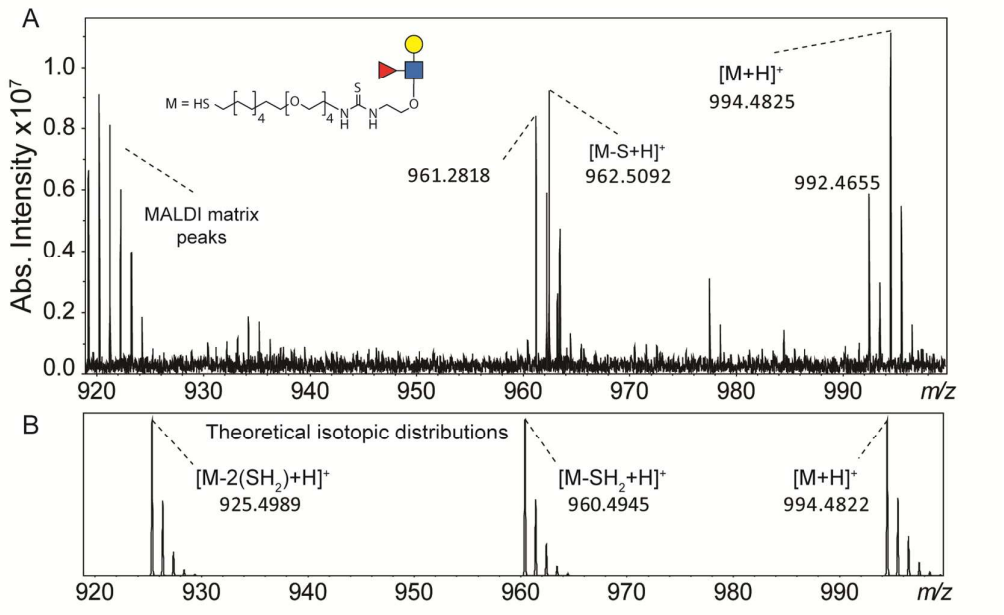

Figure S9. MALDI-FTICR spectrum of Lewis X ligand not linked to AuNPs. Contrarily to what observed in the MALDI-FTICR spectrum of Lewis X AuNPs (see Figure 4), the single and the double loss of SH_2 from $[M+H]^+$ were not observed.

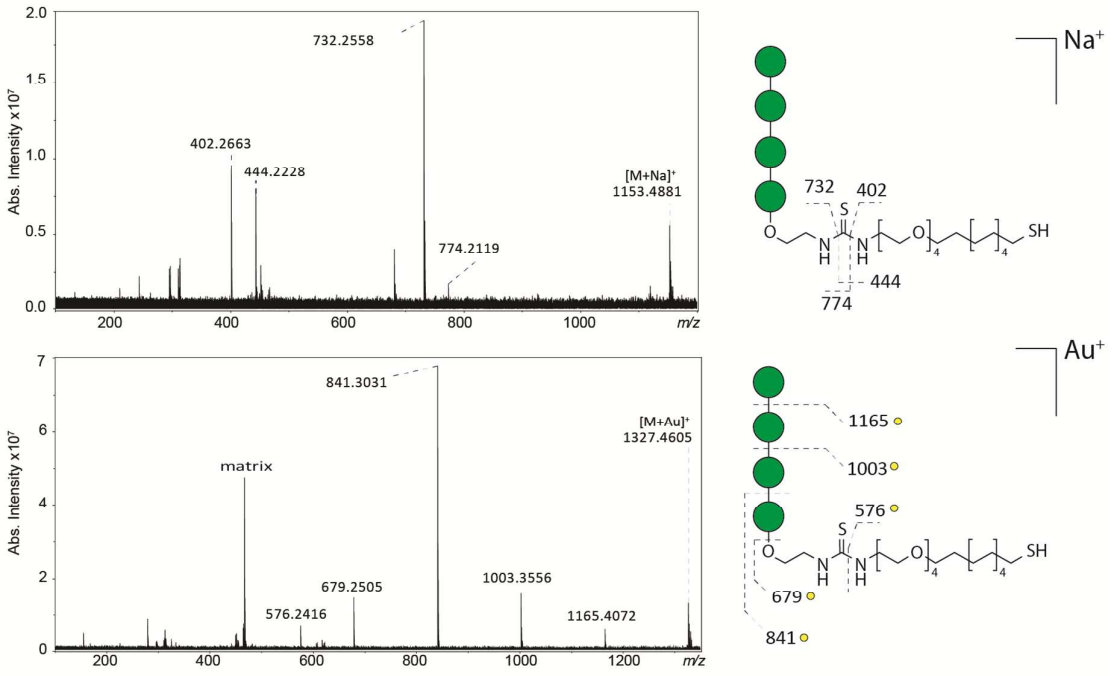

Figure S10. LDI/MALDI-CID-FTICR MS/MS spectra and structural characterization of $[M+Na]^+$ (A) and $[M+Au]^+$ (B), generated from tetramannoside AuNPs. Yellow circles indicate gold-linked fragment ions.

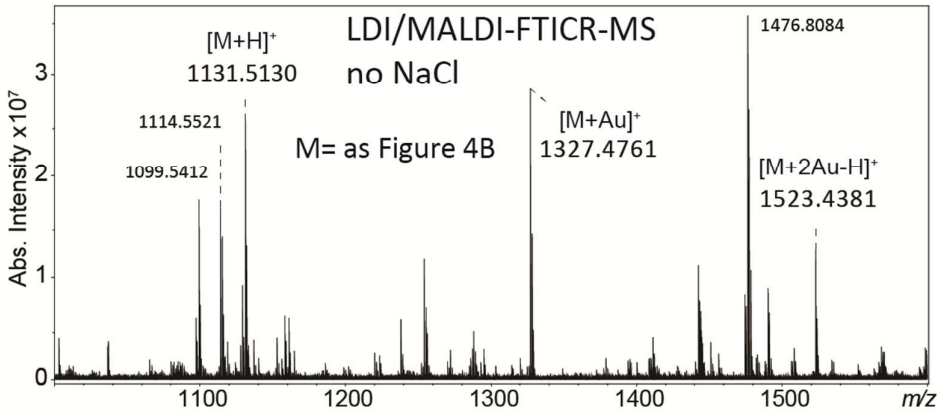

Figure S11. LDI/MALDI-FTICR MS spectrum of tetramannoside AuNPs analysed without NaCl.

Detailed experimental conditions for the synthesis of each NP and supporting structural information.

Table 1. Experimental conditions for the in situ reduction of HAuCl4 for the preparation of AuNP.

OVA peptide AuNP	umoles	Concentration (M)	eq	Volume (uL)
Organic (Thiol-ending ligands)	1,44	0,012	3	120
$HAuCl_4$	0,48	0,025	1	19
$NaBH_4$	10	1	21	10
LeX AuNP				
Organic (Thiol-ending ligands)	20,11	0,012	3	1676
$HAuCl_4$	6,7	0,025	1	268
$NaBH_4$	141	1	21	141
LeX/Tetramannoside AuNP				
Organic (Thiol-ending ligands)	5,9	0,012	3	492
$HAuCl_4$	1,97	0,025	1	79
$NaBH_4$	42	1	21	42
Tetramannoside AuNP				
Organic (Thiol-ending ligands)	17,7	0,012	3	1475
$HAuCl_4$	5,9	0,025	1	236
$NaBH_4$	124	1	21	124

AuNPs functionalized with both Lewis X and tetramannoside ligands.

Reaction of a ~2:1:10 mixture of Lewis X conjugate (*i.e.* 0.6 µmoles), Tetramannoside conjugate (*i.e.* 0.3 µmoles) and GlcC5S (*i.e.* 5 µmoles) with $HAuCl_4$ and $NaBH_4$ gave AuNPs as a dark-brown powder. Ratio between Lewis X and Tetramannoside signals ~2:1. Molar ratio of conjugates per nanoparticle was also determined by analyzing the mixtures using NMR before and after nanoparticle formation. TEM (average diameter): 1.8±0.3 nm.

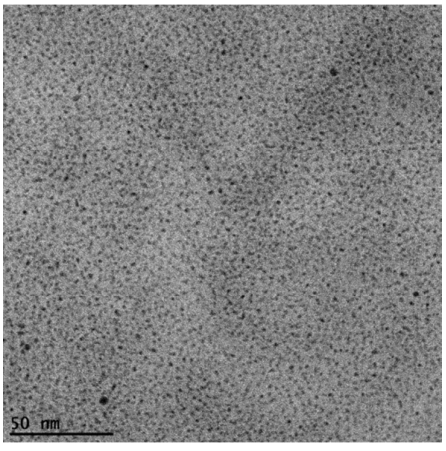

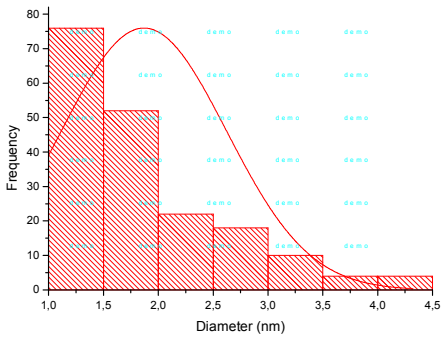

Figure S12. TEM micrograph and size-distribution histogram obtained from analysis of TEM micrographs.

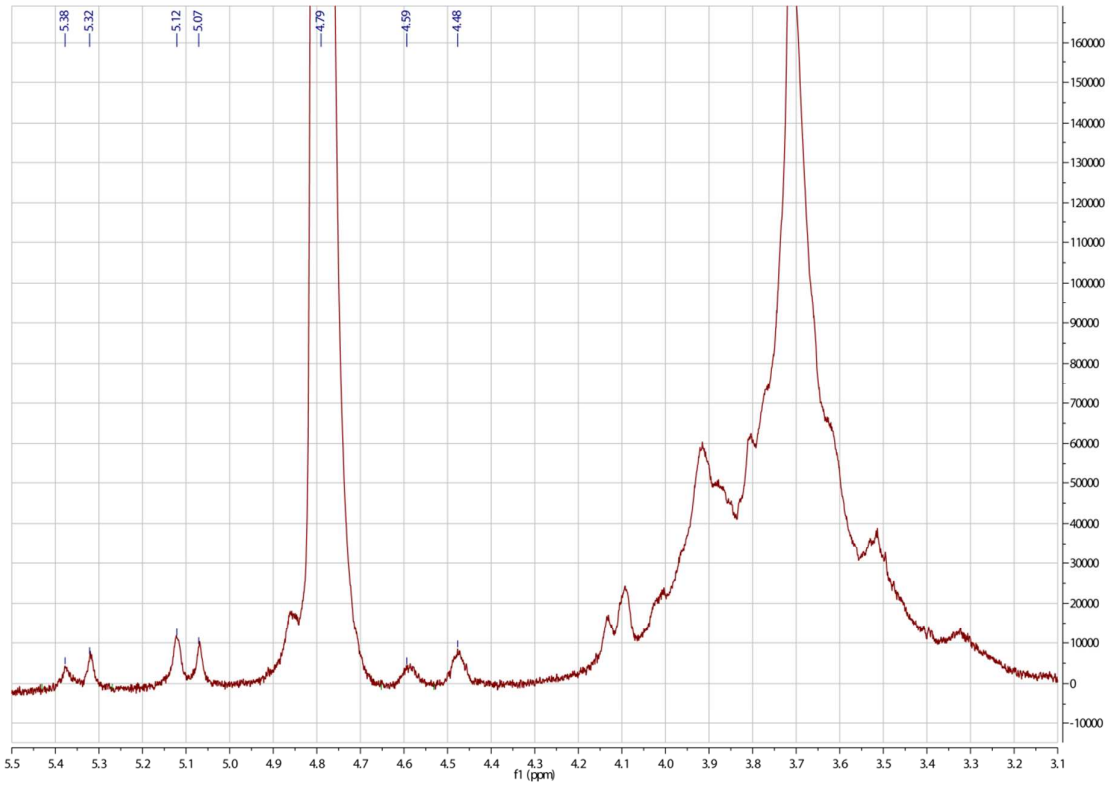

Figure S13. ^{1}H-NMR (500 MHz, D_2O) of AuNPs functionalized with both Lewis X and tetramannoside ligands. Only significant peaks are reported: δ = 5.38 (bs, from Tetramann anomeric proton), 5.32 (bs, from Tetramann anomeric proton), 5.12 (bs), 5.07 (bs), 4.59 (bs, from Lewis X anomeric proton), 4.48 (bs, from glucose anomeric proton), 2.05 (s, NAc of Lewis X conjugate), 1.20 (bs, fucose –CH_3 of Lewis X conjugate).

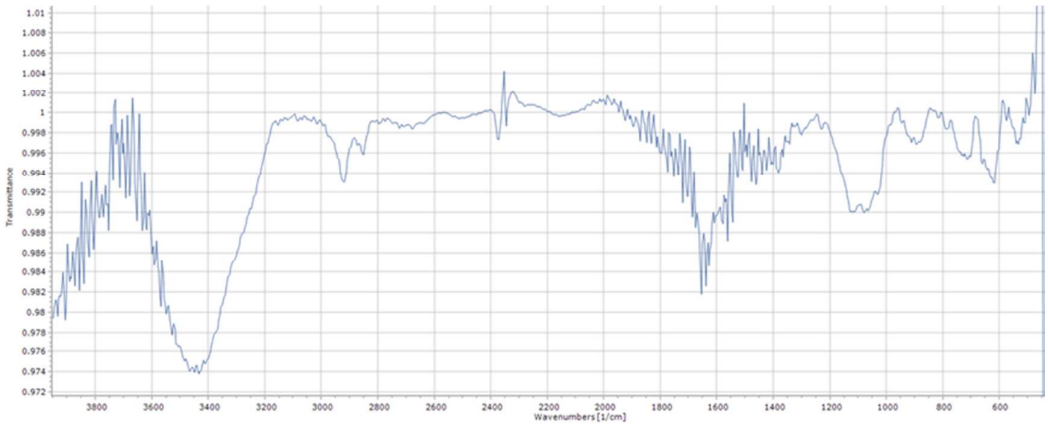

Figure S14. IR spectrum of Lewis X/tetramannoside AuNPs. IR (KBr): ν = ~3600–3100 (br), 2906, 2845, 1638, 1094.

AuNPs functionalized with Lewis X ligand.

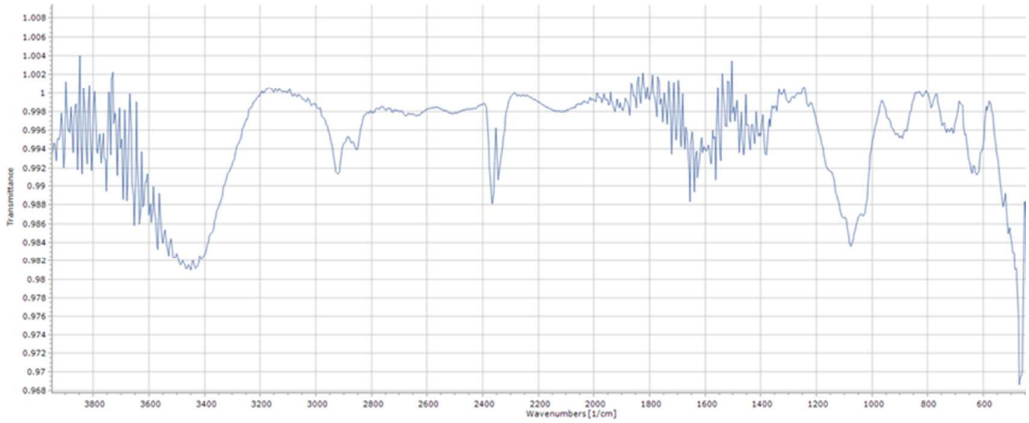

Figure S15. IR spectrum of Lewis X AuNPs. IR (KBr): ν = ~3600–3100 (br), 2919, 2848, 2365, 2343, 1654, 1381, 1069.

NMR, UV and TEM micrograph of Lewis X AuNPs have been already described in Arosio, D.; Chiodo, F.; Reina, J. J.; Marelli, M.; Penades, S.; van Kooyk, Y.; Garcia-Vallejo, J. J.; Bernardi, A., Effective Targeting of DC-SIGN by α-Fucosylamide Functionalized Gold Nanoparticles. Bioconjugate Chem. 2014, 25 (12), 2244-2251.

AuNPs functionalized with tetramannoside ligand.

NMR, UV, IR and TEM micrograph of tetramannoside AuNPs have been already described in Di Gianvincenzo, P.; Chiodo, F.; Marradi, M.; Penades, S., Gold manno-glyconanoparticles for intervening in HIV gp120 carbohydrate-mediated processes. Methods Enzymol. 2012, 509, 21-40.

AuNPs functionalized with OVA 323-339 ligand.

NMR, UV, IR and TEM micrograph of OVA 323-339 AuNPs have been already described in Safari, D.; Marradi, M.; Chiodo, F.; Th Dekker, H. A.; Shan, Y.; Adamo, R.; Oscarson, S.; Rijkers, G. T.; Lahmann, M.; Kamerling, J. P.; Penades, S.; Snippe, H., Gold nanoparticles as carriers for a synthetic Streptococcus pneumoniae type 14 conjugate vaccine. Nanomedicine-UK 2012, 7 (5), 651-62.